Underwater Target Localization using the Generalized Lloyd-Mirror Pattern

Mojgan Mirzaei Hotkani[1], Seyed Alireza Seyedin[1*], Jean-Francois Bousquet[2]
1- Department of Electrical Engineering, Ferdowsi University of Mashhad, Mashhad, Iran.
Email: seyedin@um.ac.ir (Corresponding author)
2- Department of Electrical & Computer Engineering, Dalhousie University, Halifax, NS, Canada.
Email: JBousquet@Dal.Ca.

Received: September 2020 Revised: December 2020 Accepted: February 2021

ABSTRACT:
Matched Field Processing (MFP) is one of the most famous algorithms for source detection and underwater localization. Traditional MFP relies on a match between the received signal at the hydrophone array and a replica signal, which is constructed using Green's Function, then by scanning the space in range and depth to provide an estimation of source position in shallow water and deep water. Different environment models relying on Green's function exist for constructing the replica signal; this includes normal modes in a shallow water waveguide, the Lloyd-Mirror Pattern, and the Image model. Using the proposed estimation algorithm, here, an analytical Lloyd-Mirror model is developed based on the reflection from the target surface for a case where a target is located in the source signal propagation path. So, in this paper, a new underwater acoustic target localization algorithm using the generalized Lloyd-Mirror Pattern is presented. This idea is verified using an acoustic data from a 2019 underwater communication trial in Grand Passage, Nova Scotia, Canada.

KEYWORDS: Matched Field Processing, Underwater Target Localization, Lloyd-Mirror Pattern, Normal Mode, Shallow Water, Image Model.

1. INTRODUCTION

Localization of underwater targets is of great significance and has attracted attention in the past few decades due to its growing importance in various fields such as oceanography, commercial sonar, and military applications. Generally, there are two types of localization methods; one is Matched Field Processing (MFP) that matches to the environment using a model-based approach; another is based on time-delay including multiple signal classification (MUSIC), estimation of signal parameters via rational invariance Techniques (ESPRIT), Minimum Variance Distortion Response (MVDR), Root Multiple Signal Classification (ROOT MUSIC) algorithms Multi-channel Cross-Correlation Coefficient (MCCC) that they are reviewed in [1-5]

MFP is a special beamforming technique that uses the spatial complexities of acoustic fields in an ocean waveguide to localize the active sources in range and azimuth. Also, it is a spatial filter with a correlation between the received signal and a replica, where the replica is constructed using Green's function for a waveguide [6], [7]. Green's function is used to represent the replica signal based on environmental parameters, and can be modelled using different techniques the most important of which are the normal mode for shallow water waveguide, the Lloyd-Mirror Pattern (LMP), and the Image Method [8]. The LMP occurs in underwater acoustic when the acoustic source is near the ocean surface and the ocean surface is not very rough. Using LMP interface pattern in the sound field results from constructive and destructive interface between the direct and source-reflected acoustic waves [9]. Thus, the multipath is modeled using a direct and a reflected path from the ocean surface. The constructed Green Function using the LMP has been used for active source localization.

In this paper, we propose a localization algorithm for the passive targets based on the developed LMP where a target is located in the source signal propagation path. This idea is simulated using the acoustic data from a 2019 underwater communication trial in Grand Passage, Nova Scotia, Canada.

The body of this paper is organized as follows. In Section 2, LMP is reviewed. Next, in Section 3, the experimental setup and dataset are described. Then, the

Paper type: Research paper
DOI: https://doi.org/10.52547/mjee.15.3.17
How to cite this paper: M. Mirzaei Hotkani, S. A. R. Seyedin and J. F. Bousquet, **"Underwater Target Localization using the Generalized Lloyd-Mirror Pattern"**, *Majlesi Journal of Electrical Engineering*, Vol. 15, No. 3, pp. 17-24, 2021.

proposed localization algorithm for active sources and simulation results are presented in Section 4. The Generalized Lloyd-Mirror algorithm for passive target is analyzed and simulated in Section 5. Finally, the conclusions are discussed in Section 6.

2. LLOYD-MIRROR PATTERN

As described in the introduction section, the multipath effect in LMP is modeled using both the direct and reflected paths from the ocean surface and it occurs in underwater acoustic propagation when the acoustic source point is near the ocean surface and the ocean surface is not very rough [8].

As shown in Fig. 1, "S" represents a point active source at depth "Z_s" below the ocean surface. So, the total field at any point of space *(r, z)* for two paths (direct path i.e., R_1, and the surface-reflected path i.e., R_2) can be written as

$$\psi(r,z) = S(\omega)\times\left(\frac{e^{ikR_1}}{R_1} - \frac{e^{ikR_2}}{R_2}\right), \quad (1)$$

Where, $k = \frac{2\pi}{\lambda}$ is the acoustic wavenumber, and

$$R_1 = \sqrt{r^2 + (z - z_s)^2}, \; R_2 = \sqrt{r^2 + (z + z_s)^2}. \quad (2)$$

3. EXPRIMENTAL SETUP AND DATA

The data analyzed in this paper were produced by a fishing vessel and ferry noise as well as from the vessel's sonar at frequencies of 50 kHz and 150 kHz. A potential modulated bit stream is also available in the 27-kHz range. The experiment took place on August 14, 2019, in Grand Passage, Nova Scotia, Canada. The equipment for this trial consists of three linear power amplifiers and a DC power supply to produce active signals, as well as a 5-element hydrophone array receiver with a recorder shown in Fig. 2. This array is deployed horizontally at a depth of 19.3 meters. For the receiver array shown in Fig. 2, the distance between any two adjacent corner elements is approximately 9 inches. Also, the distance from any corner element to the center element is approximately 6.5 inches.

A waterproof, pressure-resistant, battery-powered case is used to record and store data from the hydrophone array and the sampling frequency is 384 kHz. Our experimental set up is shown in Fig. 3.

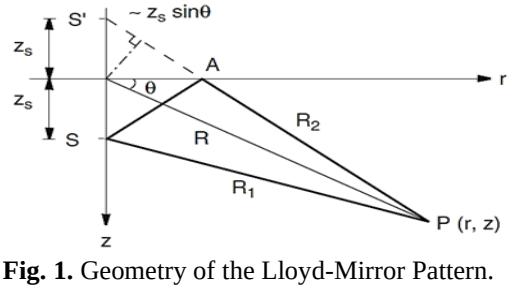

Fig. 1. Geometry of the Lloyd-Mirror Pattern.

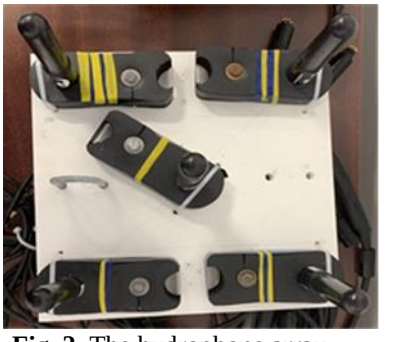

Fig. 2. The hydrophone array.

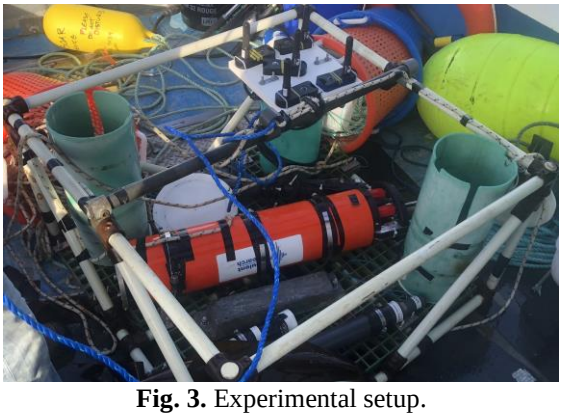

Fig. 3. Experimental setup.

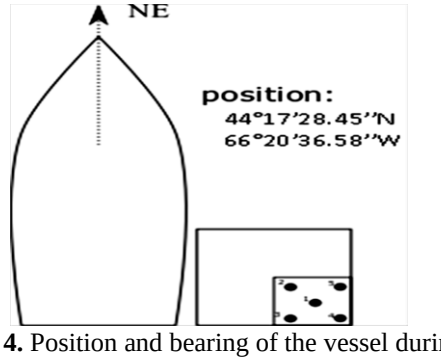

Fig. 4. Position and bearing of the vessel during deployment of the receiver.

Fig. 5. Experiment scenario and the fishing boat in the Bay of Fundy.

Ocean conditions are a very important part of this experiment. Grand Passage is a very high flow environment with rapid tides. It is situated on the southern shore of the Bay of Fundy, and it has some of the highest tides on the planet. The exact location and approximate bearing of the boat when the receiver was deployed is shown in Fig. 4. Fig. 5 shows the vessel that travelled to known positions near the array during the experiment.

This experiment is designed to support an underwater communication trial and can also be used to detect and locate the presence of a scattering target. Physical characteristics of the experiment are:

- Density of water: 1000 kg/m^3.
- Depth of sea: 20 m.
- Sound speed: 1520 m/s
- Frequency of sonar pulse: 50 kHz

4. LOCALIZATION OF ACTIVE SOURCE

In the proposed method, firstly the location of the active source must be determined by the receiver sensor. To confirm the accuracy, its location is confirmed using a GPS signal. Here, the algorithm shown in Fig. 6 is proposed for localization of the active source. The incoherent broadband MFP that estimates the source location in the proposed method relies on the eigenvalues of the cross-correlation matrix of the received signals, as defined in (3). This algorithm is summarized with the following steps:

1. Calculate the eigenvalues and the right eigenvectors of the cross-correlation matrix for the received signals, and at each discrete frequency bin.
2. Sort the calculated eigenvalues based on the absolute values of their real parts in descending order, and then sort the corresponding eigenvectors in the order of the sorted eigenvalues to produce a matrix **U**.
3. Eliminate the first eigenvector and obtain the matrix of remaining eigenvectors.
4. Multiply the **U** matrix by the computed physical model matrix Ψ based on environmental parameters with the Lloyd-Mirror model for each frequency bin.
5. Find the minimum value of the absolute value of the matrix elements obtained from the previous step, for each point in space. This is expressed as

$$(x, y, z) = \arg\min_{} \left\{ \sqrt{\sum_{f} \left(\sum_{m=2}^{M} \left| \left((u_m(f))^H \frac{\Psi(f, x, y, z)}{|\Psi(f, x, y, z)|} \right) \right|^2 \right)} \right\}, \quad (3)$$

Where, M is the number of sensors, f is the frequency, $\Psi = [\psi_1, \psi_2, \cdots, \psi_M]^H$, is the eigenvector u_i corresponding to the i^{th} sorted eigenvalue of the cross-correlation matrix of received signals for each frequency. Recall that $|.|$ and $(.)^H$ are the magnitude and Hermitian operators respectively, and ψ_i is the element of the physical model matrix that is computed by (1).

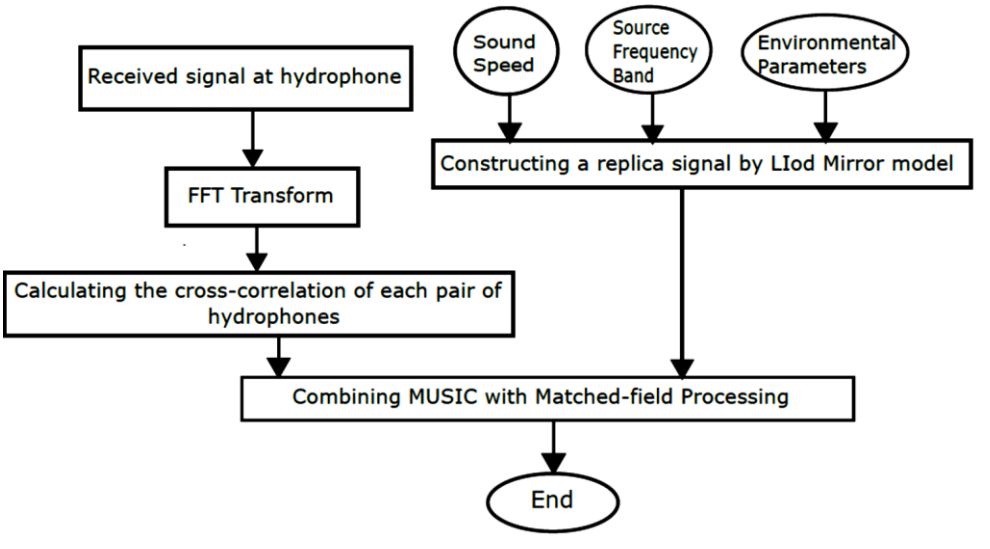

Fig. 6. The diagram of the source localization algorithm.

4.1. SIMULATION RESULTS

In this section, the localization algorithm accuracy will be assessed. The vessel sonar signal is considered as an active source signal at a frequency of 50 kHz and is placed below the vessel in this trial.

Fig. 7 shows an example of the sonar signal that is received at each hydrophone in the time-domain. Also, according to the spectrogram of the received signal shown in Fig.8, the vessel sonar can be observed in the 50 kHz band, as well as in the 150-kHz frequency band. The 50-kHz frequency is used to find the position of the vessel at any time based on the proposed algorithm that has been described in Fig. 6. The maximum energy of the ambiguity function shown in Fig. 9 shows the approximate position of the vessel at coordinates of (x=12 m, y=84 m), as computed using the proposed algorithm.

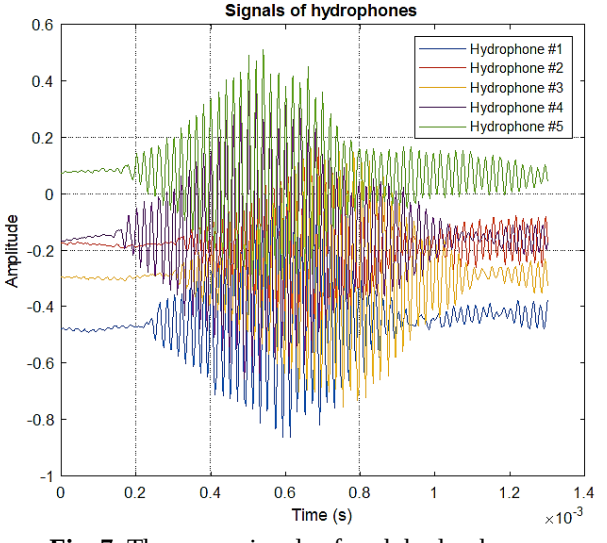

Fig. 7. The sonar signals of each hydrophone.

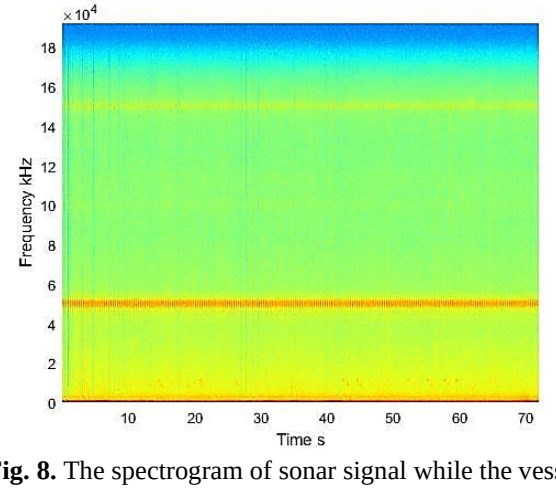

Fig. 8. The spectrogram of sonar signal while the vessel was moving away from the receiver.

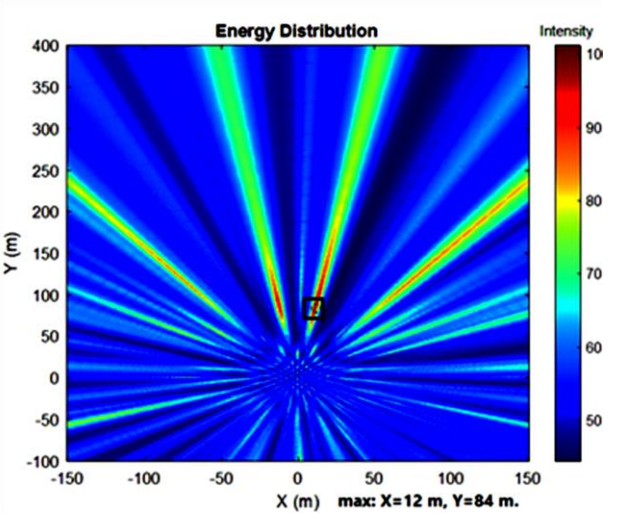

Fig. 9. The ambiguity figure of the boat localization.

A preliminary analysis of the data showed the presence of various species of animals, including harbor porpoises and humpback whales; echolocation patterns in different frequency bands were observed. Next, we intend to use the clicks of harbor porpoise to localize the animal using the proposed source localization algorithm.

The harbor porpoise, *Phocoena phocoena*, is one of seven species of porpoise. It has about 1.5 m long and weighting around 65 kg. They emit narrowband ultrasonic signals at high frequency. Their clicks are centered between 130 to 140 kHz with a bandwidth of 6 to 26 kHz and the duration of the clicks are about 44–113 µs. They use echolocation to hunt fish; after sending the signals, they listen for the faint echoes returned from fish [10], [11].

Fig. 10 shows the harbor porpoise click that was observed in the Bay of Fundy at a frequency of 140 kHz.

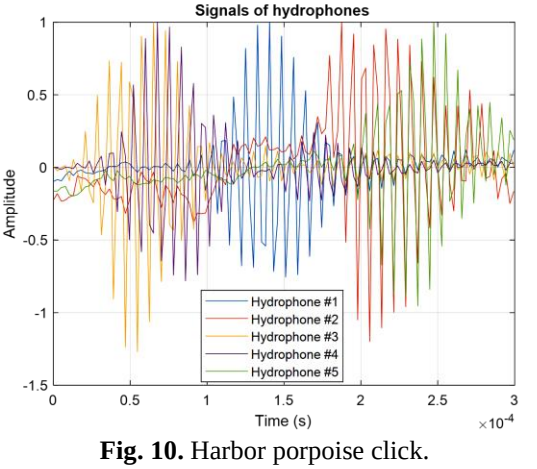

Fig. 10. Harbor porpoise click.

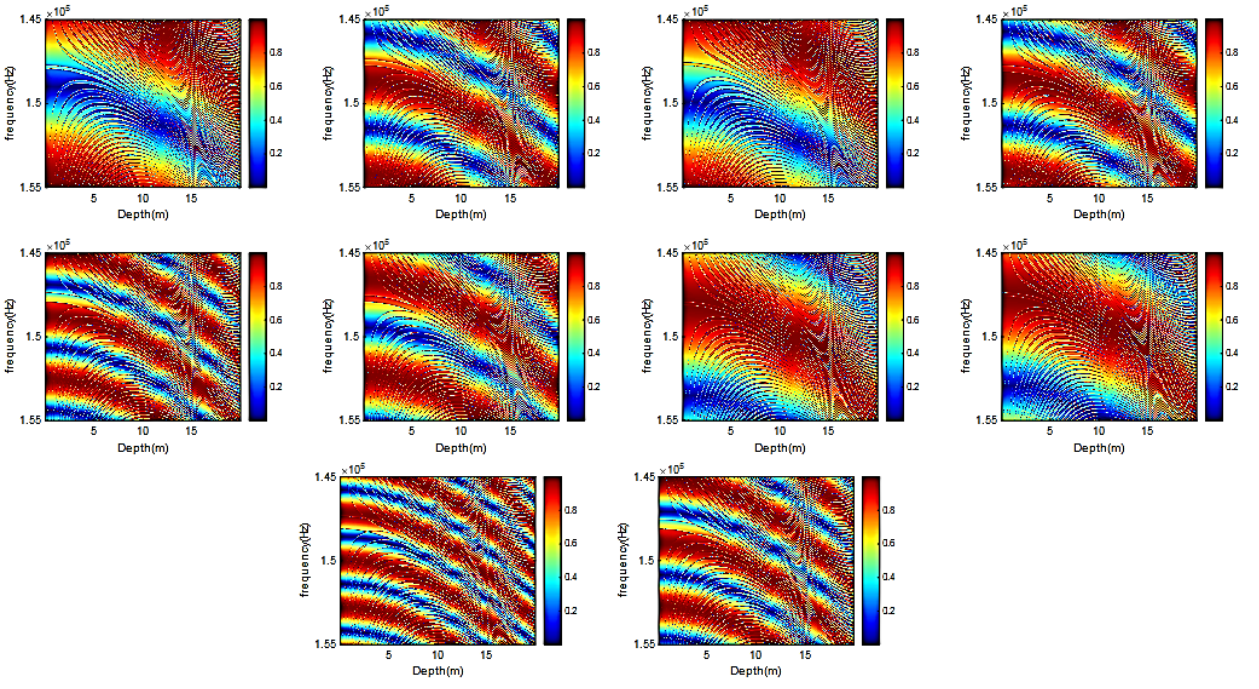

Fig. 11. Investigation of the magnitude changes in the imaginary part of the Lloyd-mirror model as function of frequency and depth at a specific range and azimuth.

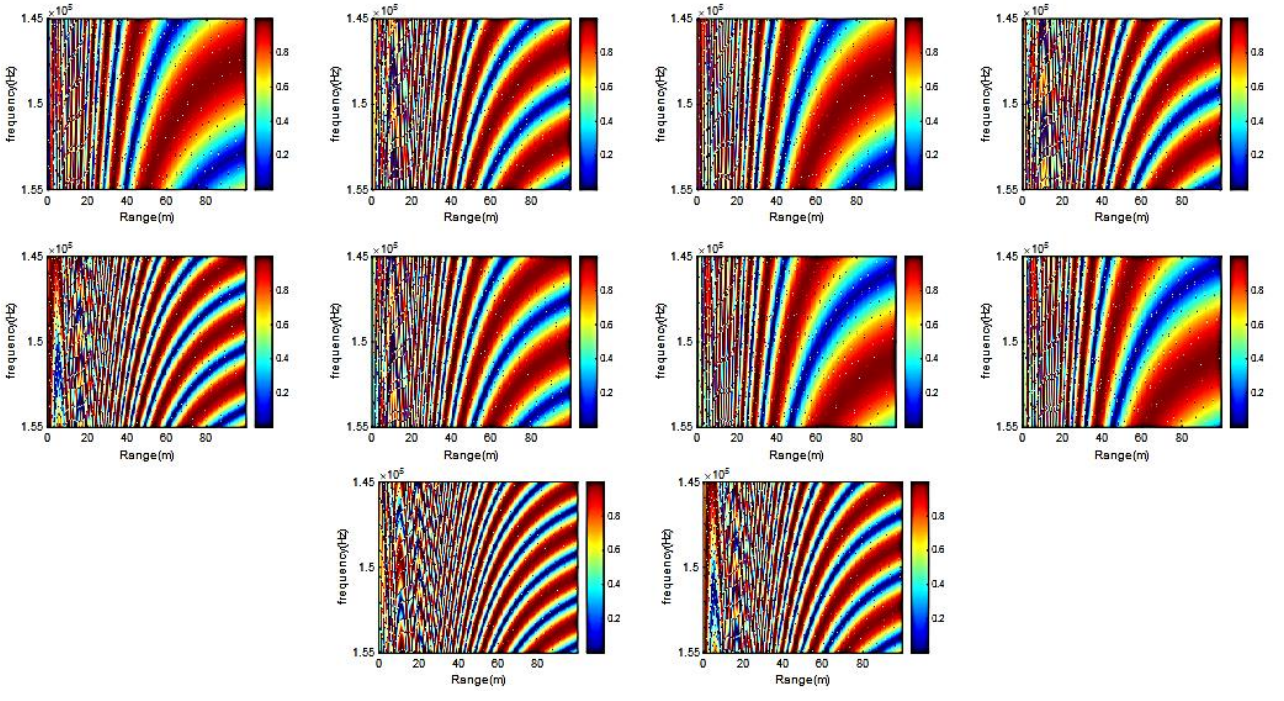

Fig. 12. Investigation of the magnitude changes in the imaginary part of the Lloyd-mirror model as function of frequency and range at a specific depth and azimuth.

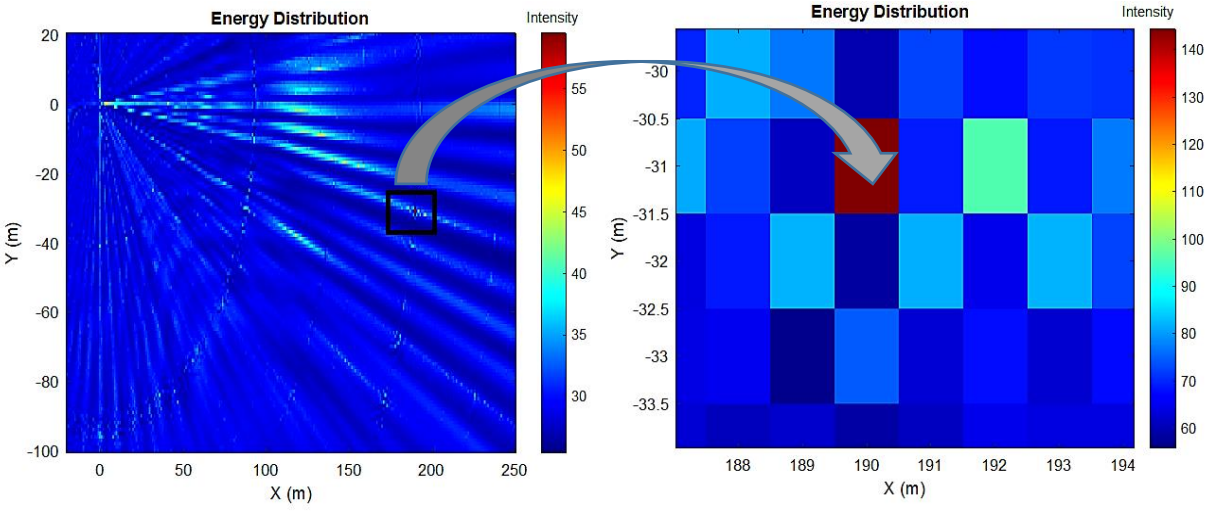

Fig. 13. Estimated harbor porpoise's location by applying the Lloyd-Mirror model combined with MUSIC algorithm (The figure on the right is zoomed in on the target area).

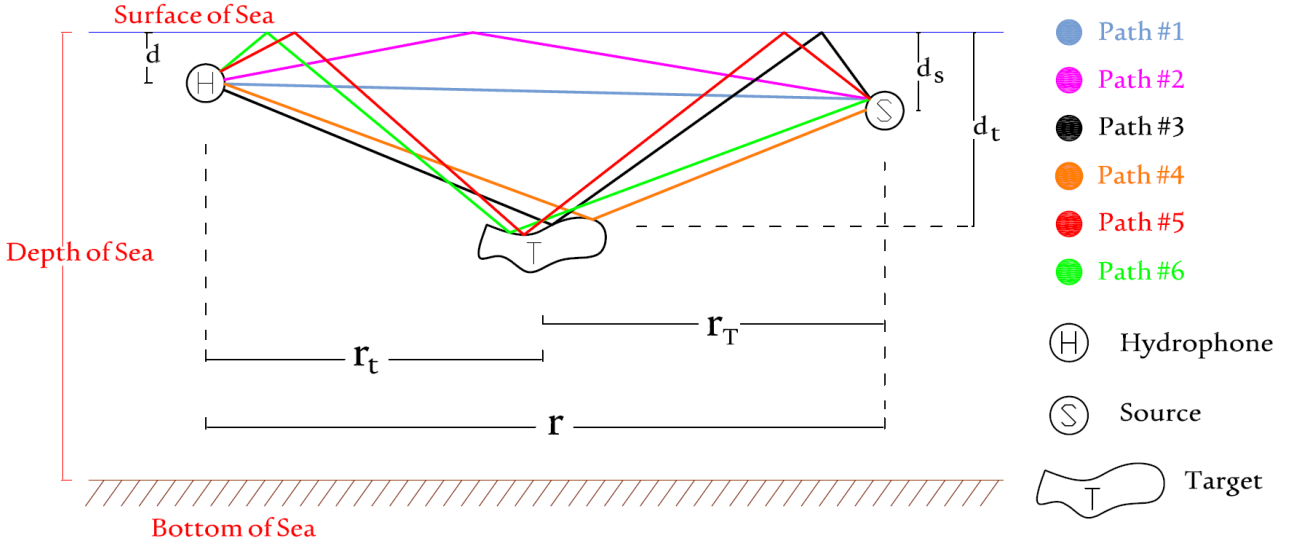

Fig. 14. Schematic of proposed model.

Since the produced clicks by harbor porpoises are at high frequency, it is very likely that aliasing will occur. By simulating and analyzing the Lloyd-mirror model in the frequency domain as shown in Fig. 11 and Fig. 12, the intensity of the magnitude changes for this model can be seen in terms of frequency, range, and depth. Each of the sub-figures shows the result of cross-correlation of the modeled signal between each hydrophone with other ones, i.e. $[P_1P_2^T, P_1P_3^T \ldots P_4P_5^T]$ from left to right.

According to all cross-correlation patterns shown in Fig. 12, in the frequency band related to the signal generated by the harbor porpoise, there is a sharp change for a range smaller than 30 meters, and aliasing has occurred. Also, Fig. 13 shows the estimated harbor porpoise's location by applying the Lloyd-Mirror model combined with MUSIC algorithm.

5. GENERALIZED LLOYD-MIRROR PATTERN

Using Lloyd's geometry, if a target is added to the environment, six paths will be created as depicted in Fig. 14. According to the Lloyd's equation, the propagation model is generalized to (4).

$$P_h = P_1 + P_2 + P_3 + P_4 + P_5 + P_6, \quad (4)$$

Where, P_i is the scattered power strength in each path between the source and the receiver. Therefore,

additionally to the paths that scatter from the target, there are four paths that arrive indirectly (i.e. the paths number 3, 4, 5 and 6 as shown Fig. 14) in the hydrophone array, in addition to the direct path (i.e. the path number 1 in Fig. 14) and the reflected path from the ocean surface (the path number 2 in Fig. 14). So, the i^{th} path contains a delay of kR_i and an attenuation factor of $\frac{1}{R_i}$. Therefore, the field at each path can be written as $\frac{e^{-jkR_i}}{R_i}$. According to Fig. 14, we have

$$\begin{cases} P_1 = \dfrac{e^{jk\sqrt{r^2+(d-d_s)^2}}}{\sqrt{r^2+(d-d_s)^2}} \\ P_2 = K_2 \dfrac{e^{jk\sqrt{r^2+(d+d_s)^2}}}{\sqrt{r^2+(d+d_s)^2}} \\ P_3 = K_3 \dfrac{e^{jk\left(\sqrt{r_T^2+(d_t+d_s)^2}+\sqrt{r_t^2+(d-d_t)^2}\right)}}{\left(\sqrt{r_T^2+(d_t+d_s)^2}+\sqrt{r_t^2+(d-d_t)^2}\right)} \\ P_4 = K_4 \dfrac{e^{jk\left(\sqrt{r_T^2+(d_s-d_t)^2}+\sqrt{r_t^2+(d-d_t)^2}\right)}}{\left(\sqrt{r_T^2+(d_s-d_t)^2}+\sqrt{r_t^2+(d+d_t)^2}\right)} \\ P_5 = K_5 \dfrac{e^{jk\left(\sqrt{r_T^2+(d_t+d_s)^2}+\sqrt{r_t^2+(d+d_t)^2}\right)}}{\left(\sqrt{r_T^2+(d_t+d_s)^2}+\sqrt{r_t^2+(d+d_t)^2}\right)} \\ P_6 = K_6 \dfrac{e^{jk(\sqrt{r_T^2+(d_t-d_s)^2}+\sqrt{r_t^2+(d+d_t)^2})}}{(\sqrt{r_T^2+(d_t-d_s)^2}+\sqrt{r_t^2+(d+d_t)^2})} \end{cases} \quad (5)$$

Note that the coefficients K_i are obtained according to the following boundary conditions:

1. The sound pressure at the ocean surface is equal to zero.
2. The target is in the direct path between the source and the receiver.
3. The target is in each of the reflected paths.

Therefore:

1: If d=0 $\Rightarrow P_{h=0}=0 \Rightarrow \{\boxed{K_2=-1},\ \boxed{K_3=-K_5},\ \boxed{K_4=-K_6}\}$.

2: If the target is located on the path #1

$$\Rightarrow \begin{cases} \text{Path}_1 = \text{Path}_4 \\ P_h = P_2 + P_3 + P_5 + P_6 \end{cases},$$

$$\Rightarrow \{P_1 + P_4 = 0 \Rightarrow \boxed{K_4=-1} \Rightarrow \boxed{K_6=1}. \quad (6)$$

3: If the target is located on the left part of path #2:

$$\Rightarrow \begin{cases} \text{Path}_2 = \text{Path}_3 \\ P_h = P_1 + P_4 + P_5 + P_6 \end{cases}$$

$$\Rightarrow \{P_2 + P_3 = 0 \Rightarrow \boxed{K_3=1} \Rightarrow \boxed{K_5=-1}. \quad (7)$$

5.1. SIMULATION RESULTS

In Section 4, the position of the active source at the coordinates of (x=12 m, y=84 m) was estimated using the sonar. Now, given this position and simulating the set of Equations (4) to (7) by sweeping the space at a depth of 19.8 m in the ocean, Fig. 15 was obtained. Note that the pressure capsule (shown in Fig. 3) is considered as the target. The Zone 1 in Fig. 15 shows the maximum energy associated with the reflection from the target surface.

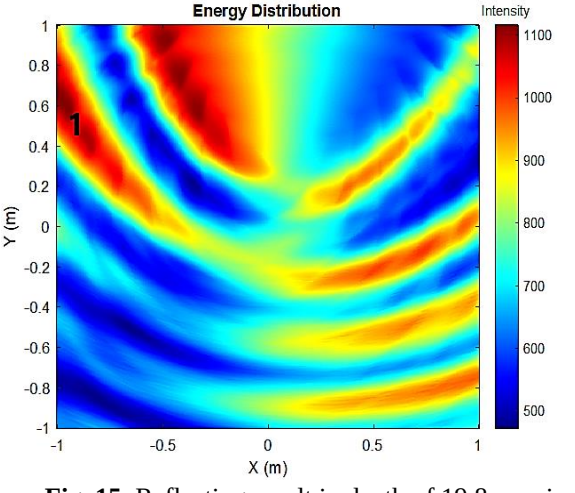

Fig. 15. Reflecting result in depth of 19.8 m using the proposed algorithm.

6. CONCLUSION

In this paper, we proposed an algorithm for localizing the passive underwater targets using an active source that has a position that was already estimated using Matched Field Processing (MFP) and an eigenvector-based estimator. The propagation of underwater acoustics causes adverse effects of multipath, and this has been modeled according to LMP. Also, it was necessary to define a replica signal based on environmental parameters in order to localize the passive underwater targets using MFP, and we derived a model according to the generalized LMP with specific boundary conditions to generate the replica signal. This idea was demonstrated with real acoustic data using a fishing vessel sonar deployed in Grand Passage, Nova Scotia. Also, we utilized the proposed localization algorithm to find the position of the harbor porpoises in Grand Passage. Since these animals emit ultrasonic signals high frequency, aliasing occurs. Instead, LMP combined with MUSIC can detect the position of the harbor porpoise with minimal aliasing effects.

REFERENCES

[1] H. Tang, **"DOA estimation based on MUSIC algorithm,**" *thesis Basic level (degree of Bachelor), Linnaeus University*, Department of Physics and Electrical Engineering, 2014.

[2] C. Qian, L. Huang, and H. C. So, **"Improved unitary root-MUSIC for DOA estimation based on pseudo-noise resampling,"** *IEEE Signal Process. Lett*. 2014.

[3] W. Suleiman, M. Pesavento, and A. M. Zoubir, **"Performance Analysis of the Decentralized Eigen decomposition and ESPRIT Algorithm**,**"** *IEEE Trans. Signal Process.*, 2016.

[4] J. Benesty, J. Chen, and Y. Huang, **Microphone array signal processing**. *Springer*, 2008.

[5] M. Mirzaei Hotkani, S. A. Seyedin, and J. F Bousquet, **"Underwater Object Localization using the Spinning Propeller Noise of Ships Based on the Wittekind Model"** *International Journal of Engineering and Advanced Technology*, pp. 2736-2741, 2020.

[6] P. N. Tran and K. D. Trinh, **"Adaptive Matched Field Processing for Source Localization Using Improved Diagonal Loading Algorithm,"** *Acoust. Aust*., 2017.

[7] A.B. Baggeroer, **"Matched field processing: source localization in waveguides"** Proceedings Article, *the Twenty-Sixth Asilomar Conference on Signals, Systems & Computers*, 1992.

[8] J. Engelbrecht, A. Guran, G. A. Maugin, M. Werby, **Acoustic Interactions with Submerged Elastic Structures**. *World Scientific*, Jul. 31, 2001.

[9] F. B. Jensen, W. A. Kuperman, M. B. Porter, **Computational Ocean Acoustics,** *Springer*, 2011**.**

[10] L. A. Miller, M. Wahlberg, **"Echolocation by the harbour porpoise: life in coastal waters,"** *Frontiers in Physiology.* 2013.

[11] https://www.americanscientist.org/article/the-acoustic-world-of-harbor-porpoises.

[12] R. J. Urick, **"Principles of underwater sound",** *McGraw-Hill***,** 1983.